

Simulations of a G protein-coupled receptor homology model predict dynamic features and a ligand binding site

Steffen Wolf^a, Marcus Böckmann^{a,b}, Udo Höweler^c, Jürgen Schlitter^a, Klaus Gerwert^{a,*}

^a Department of Biophysics, University of Bochum, ND 04 North, 44780 Bochum, Germany

^b Department of Theoretical Chemistry, University of Bochum, 44780 Bochum, Germany

^c CHEOPS Molecular Modelling, 48341 Altenberge, Germany

Received 14 March 2008; revised 7 July 2008; accepted 24 August 2008

Available online 5 September 2008

Edited by Robert B. Russell

Abstract A computational approach to predict structures of rhodopsin-like G protein-coupled receptors (GPCRs) is presented and evaluated by comparison to the X-ray structural models. By combining sequence alignment, the rhodopsin crystal structure, and point mutation data on the β_2 adrenoceptor (b2ar), we predict a (–)-epinephrine-bound computational model of the β_2 adrenoceptor. The model is evaluated by molecular dynamics simulations and by comparison with the recent X-ray structures of b2ar. The overall correspondence between the predicted and the X-ray structural model is high. Especially the prediction of the ligand binding site is accurate. This shows that the proposed dynamic homology modelling approach can be used to create reasonable models for the understanding of structure and dynamics of other rhodopsin-like GPCRs.

© 2008 Published by Elsevier B.V. on behalf of the Federation of European Biochemical Societies.

Keywords: Molecular dynamics simulation; GPCR; Homology model; Beta(2) adrenoceptor; Epinephrine; Ligand binding

1. Introduction

GPCRs form the largest group of membrane receptors and share a common structural motif of seven transmembrane α -helices (7TM domain) [1]. Members of this protein family are the target of more than 50% of drugs sold worldwide [2]. Milestones in understanding of their molecular reaction mechanisms are the determinations of the X-ray structures for two GPCRs: the visual receptor rhodopsin [3,4], and very recently the β_2 adrenoceptor (b2ar) [5,6]. The rhodopsin structures stimulated theoretical studies in which it was used as the major template to explore structural features and mechanisms of class A receptors [1,7–10], including b2ar [11–14] and other GPCRs. Our goal here is to set up computational models of class A GPCRs via homology modelling. They should provide insight into their structure and dynamic properties in biological membranes via unrestrained (free) molecular dynamics (MD) simulations. So far, this goal has been approached in various ways [15–19], but due to the lack of information on a second GPCR structure, the accuracy of the structure prediction was unable to be assessed. The recent publication of the first b2ar crystal structure now allows us to evaluate such GPCR modelling procedures.

In the presented approach we combine binary and multiple sequence alignment, structural features of rhodopsin and point mutation data on (–)-epinephrine-b2ar interaction [20] to create a homology model, called B2AR, which is subjected to free MD simulations in an explicit membrane/solvent environment. In contrast to docking of ligands into static homology models [11–14] or static models from frames out of MD simulations [16–19], B2AR contains an epinephrine molecule in our approach during the whole simulation period. In so doing we want to evaluate the quality of possible binding modes proposed by experimental data [20]. We then evaluate structural, functional and epinephrine binding features of the dynamic model by comparison with the human b2ar crystal structures. As the two structures available are rather similar, we focus on the comparison with the PDB structure 2RH1 [6], which is the one with the highest resolution.

2. Materials and methods

2.1. Sequence alignment

Rat b2ar (UniProtKB accession number P10608) was subjected to binary alignment with bovine rhodopsin (P02699) using BLAST (BLOSUM62 matrix) [21]. For the additional multiple sequence comparison with ClustalW [22], the class A GPCR sequences P34971, P30546, P08911, and Q9H205 were included in the alignment. The binary alignment was used as the basis for modelling. The multiple alignment was used to cross-check if motives found to be conserved in the binary alignment could be regarded as being modular. Sequence parts with the same results in both alignments and containing the highest conserved helical residues [23] were defined as “anchor groups”. Gaps within helical regions were moved to loop regions by shifting the sequence towards the next anchor group. Furthermore intraprotein hydrogen bonds and salt bridges, and the positioning of positive charges (Arg, Lys, His) at the level of phosphate groups within the membrane were taken into consideration as structural restraints. Hydrophilic residues within the heptahelical transmembrane domain were placed at positions in which they were oriented towards the protein core. The sequence of extracellular loop 2 (el2) was shifted to allow the formation of a disulphide bond between Cys106 (helix III) and Cys184 (el2), as seen in the rhodopsin crystal structures. Due to their structural importance for the C-terminal end of helix VI and the el2, substitution of Trp175 and Arg177 by analogous residues Trp173 and Arg175 was ensured. As small ligand binding and structural changes during activation take place within the 7TM domain [24–26], N-/C-terminal domains and intracellular loop 3 (il3) were left out for modelling.

2.2. Homology modelling

Chain A of rhodopsin crystal structure 1U19 [4] was used as a basis structure. Internal water molecules were ignored during model building. As palmitoyl residues at the end of helix VIII are located on the protein surface, forming the protein dimerisation interface [6], and

*Corresponding author. Fax: +49 234 3214626.
E-mail address: gerwert@bph.rub.de (K. Gerwert).

glycosylations do not influence the ligand binding of b2ar [27], post-translational modifications were not taken into account for modelling. Sequence replacement was performed with SCWRL [28]. Remaining sterical clashes were removed with MOBY [29]. Sequence gaps/inserts in the loop regions were resolved by addition/removal of amino acids, followed by short periods of simulated annealing (5 ps), energy minimisation of the respective loops and full model minimisation.

2.3. Addition of epinephrine

The minimal energy structure and atomic charges of epinephrine were determined by GAUSSIAN03 [30] vacuum DFT calculations with B3LYP/6-31++G(d,p) and RESP atomic charges calculation [31]. The protein model was checked for internal cavities with MOBY. Epinephrine in its vacuum minimal energy structure was placed into the only cavity large enough to contain the ligand according to hydrogen bond contacts determined in point mutation analysis [20]. These contacts were: Asp113/ammonium moiety; Asn293/ β hydroxyl group; Ser203, Ser204/meta hydroxyl group; and Ser207/para hydroxyl group. Epinephrine was subjected to a molecular mechanics steepest descent minimisation with distance restraints on polar residues in protein side chains and ligand mentioned above, followed by minimisation of the ligand plus surrounding residues within 4 Å. The resulting protein/ligand model was used in the following MD simulations.

2.4. Molecular mechanics simulations and data analysis

Simulations were carried out with GROMACS 3.3 [32] by merging the GROMOS96 force field and lipid parameters of Berger et al. [33,34] according to Schlegel et al. [9]. All acidic/basic side chains were fully charged except Asp79, which is protonated in rhodopsin [35]. A topology for (-)-epinephrine was obtained from the PRODRG server [36] with the atomic charges mentioned above. The protein/ligand model was introduced into an equilibrated bilayer of 256 POPC molecules, surrounded by a 154 mM NaCl solution, following the procedure of Kandt et al. [37]. The resulting system contains 68770 atoms. After system equilibration, trajectories with a length of 10 ns were recorded. An analysis of the trajectories (energies, root mean square displacement (RMSD) and fluctuations (RMSF) of atom coordinates) was performed using GROMACS [29] and MOBY [32] analysis tools. The root mean square (RMS) deviation of the crystal structure 2RH1 was calculated from the B factors given in the crystal structure file by

$$\sigma_i = \sqrt{\frac{B_i}{8\pi^2}}$$

with σ being the root mean square deviation of the position of atom i , and B the respective B factor.

3. Results

3.1. Equilibration of model structure

Analysis by MOBY confirmed that the total system energy (E_{tot}) dropped to its final value during unrestrained MD simulation after 6 ns. The total energy of the protein (E_{prot}) reached a minimum after 8 ns. The seven transmembrane helices remained within an C_α atom RMSD of 2.3 Å from the starting structure. In comparison to 2RH1, it rose to an average value of 2.5 Å within 1 ns, and climbed only slightly to an average value of 2.8 Å after 7 ns. Because of the C_α -RMSD comparison with 2RH1, we took the last 3 ns of the trajectory into account for further analysis. During this period, the loop regions showed pronounced movements with a resulting root mean square fluctuation (RMSF) of C_α atom coordinates of 1.2–2.0 Å, while the transmembrane helices remained stable in position (RMSF of 0.5–0.8 Å).

3.2. Comparison of X-ray and model structure

In Fig. 1 the X-ray structure and the mean 3-D structure of our B2AR model during the last 3 ns of MD simulation are compared with each other. The RMSD resolved for each C_α atom of the modelled structure is shown. A high correspondence is found for the positions of the seven transmembrane helices (I–VII). One hundred and thirty eight of 198 (70%) C_α atoms of the transmembrane helices are within 2.0 Å of the crystal structure. Thereof 75 (38%) are within the RMS deviation calculated from the B factors of atom coordinates in the crystal structure and thus within the statistical significance of the 2RH1 coordinates (error bar of the B2AR model in Fig. 1 contains the RMS deviation curve of the b2ar crystal structural model). They are mostly located in the middle of the helical bundle. Furthermore, the additional helix VIII

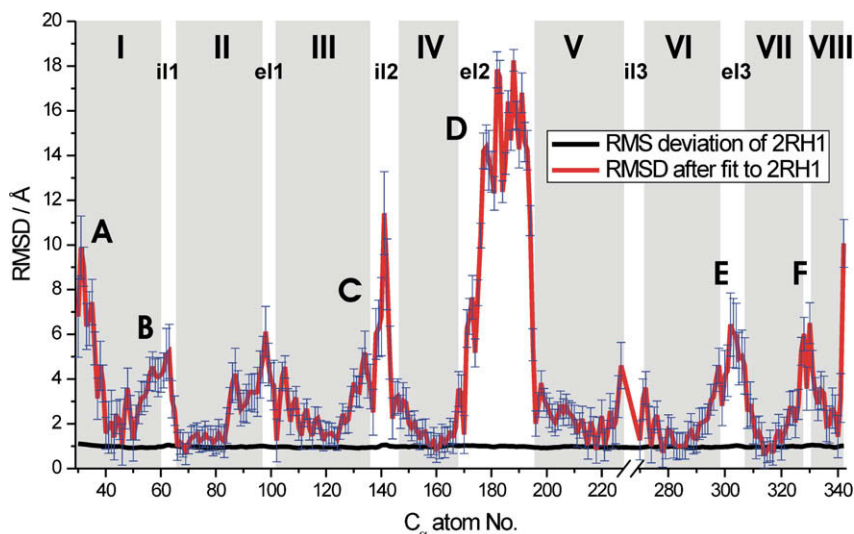


Fig. 1. Root mean square displacement (RMSD) of the modelled B2AR structure from 2RH1 for each C_α atom (red) during last 3 ns of MD simulation compared to the respective root mean square (RMS) deviation of 2RH1 calculated from B factors of the crystal structure (black). The root mean square fluctuation (RMSF) of the respective B2AR model atom coordinates, equalling the RMS deviation of the coordinates during simulation, is shown as blue error bars. Positions of the helices highlighted in grey. Letters A–F refer to sites shown in Fig. 2. The 7TM motif closely resembles the crystal structure.

[3,6] is identified and within max. 3.0 Å of the b2ar crystal structural model.

As can be seen in Fig. 2A, the remaining 30% of the helices where there was no match between the model and the X-ray structure mostly correspond to protein parts with interprotein contacts, which artificially stabilise the protein in the crystal. Such positions (denoted A–F in Figs. 1 and 2) cluster at the extracellular ends of helices I (A) and VI (E), and the intracellular ends of I (B), III (C), and VII (F). While contacts B and F connect two proteins in the proposed b2ar dimer [6], A is formed between two b2ar proteins not engaged in a dimer. C and E are formed between b2ar and neighbouring T4 lysozyme portions of the fusion protein. For a more detailed comparison of the tertiary structure of the two adrenergic receptor models, their 3-D structures are superposed in Fig. 2B–D. In comparison with the crystal structure, helix I shows a tilt of 33° at the extracellular and 13° at the intracellular half, with Ile43 being the centre of rotation, leading to a positional deviation of 10 Å of the extracellular and 5 Å of the intracellular end. Further shifts in positions away from their corresponding 2RH1 positions can be observed for the extracellular ends of II (5 Å outward movement), III (4 Å inward movement), VI (4 Å inward movement) and VII (4 Å outward movement) and the intracellular ends of III (4 Å inward movement) and VII (5 Å outward movement). The tilting movement of helix I is followed by a shift of the extracellular end of II and the intracellular end of helix VII, leading to their deviation from the crystal structure. Although the il3 is missing, the intracellular ends of helices V and VI remain within 4 Å of and therefore close to 2RH1.

As expected, larger deviations are observed for the loop regions (extracellular loops (el) 1–3 and intracellular loops (il) 1–3), but remain reasonably close to the crystal structure. One exception is el2, which is displaced by up to 20 Å (peak D in Fig. 1). As we start with rhodopsin as the basis structural information, the loop is present as a β hairpin which enters deep into the protein core. As a result, the disulphide bond observed in rhodopsin between el2 and helix III is reproduced in the model by connecting Cys106 (helix III) and Cys184 (el2). However, crystal structure [6] and point mutation analysis of b2ar [38] point to two disulphide bonds, one between Cys106/Cys191, and the other between Cys184/Cys190. Because the disulphide bonds are not correctly recognized in the model, the el2 seems thus incorrectly predicted, which causes the largest deviation between model and X-ray structure. In 2RH1, the el2 forms a helix on top of the binding crevice instead of the β hairpin deep inside the rhodopsin molecule. However, the el2 forms various contacts to the T4 lysozyme portion of neighbouring proteins within 2RH1 (contact D in Fig. 2), and thus may not reveal its native structure in the crystal structure. In addition, the loop is not observed in the second crystal structure available [5] because of local disorder. Due to its disulphide link to the el2, the modelled extracellular top of helix III shows a shift in position relative to 2RH1 as well.

3.3. Dynamic features

In Fig. 3 features of the modelled structure, which are elucidated by dynamics, are shown in detail. The model exhibits a stable interhelical hydrogen bond between the highly conserved

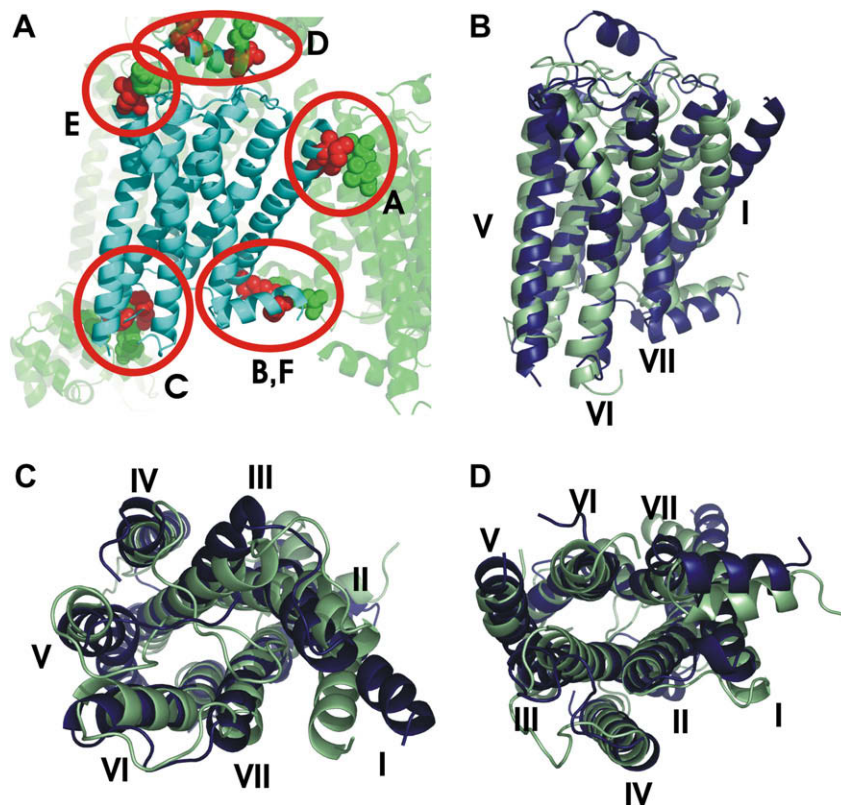


Fig. 2. (A) Interprotein contacts in the crystal structural model. Peak positions A–F in Fig. 1 coincide with crystal contacts in 2RH1 close to the 7TM motif. (B–D) Comparison of b2ar crystal structure and mean model structure during last 3 ns of MD simulation: side (B), extracellular (C) and intracellular (D) view. 2RH1 in blue, mean structure of the dynamic model in green.

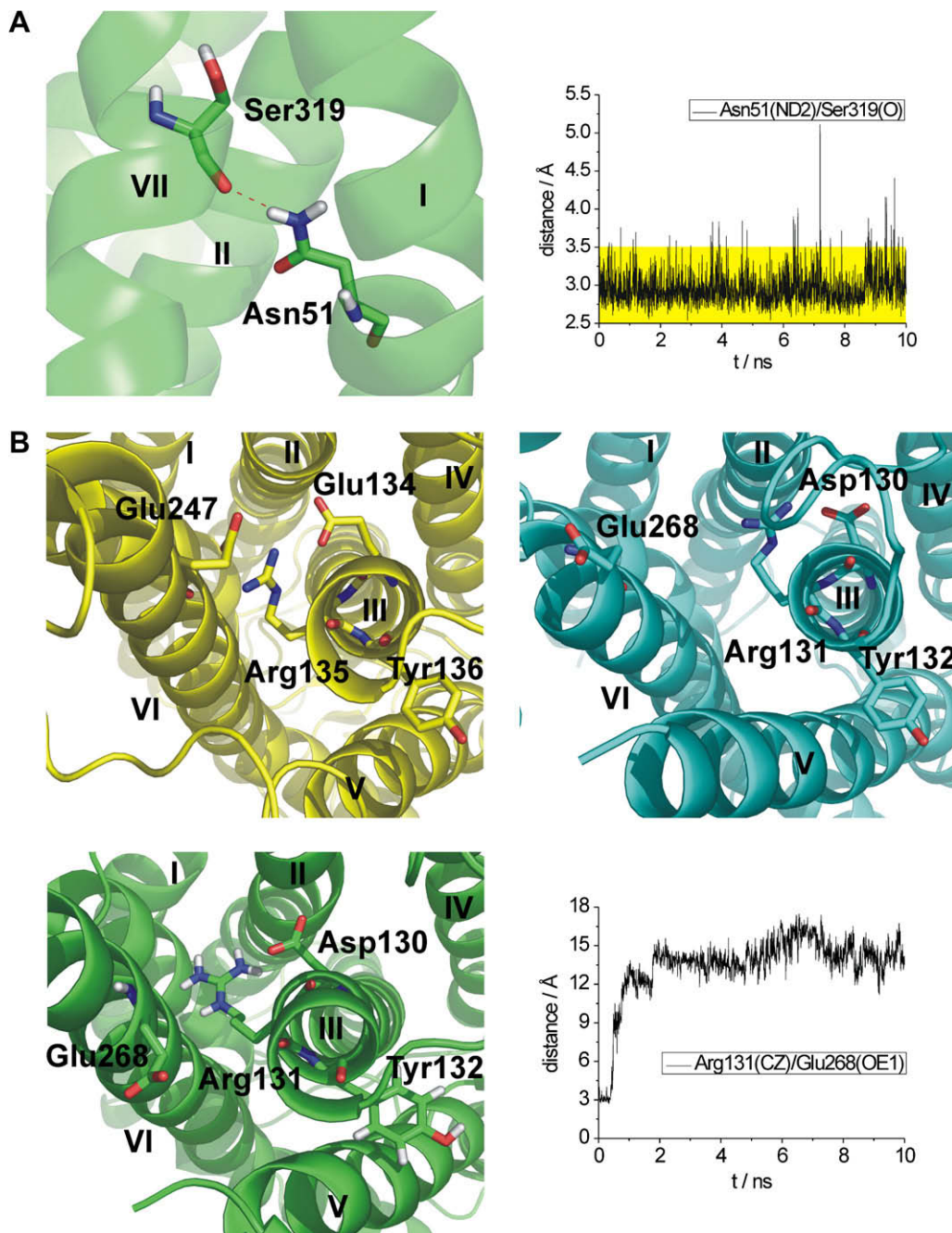


Fig. 3. (A) Interhelical contact between Asn51 and Ser319 during free MD simulation. Right: Distance of hydrogen bond donor/acceptor atoms. Hydrogen bond distances highlighted in yellow. The bond remains stable during simulation. (B) Comparison of ionic lock motifs. Top left: rhodopsin crystal structure 1U19. Top right: b2ar crystal structure 2RH1. Bottom left: Model after 1.5 ns MD simulation. Bottom right: Distance plot of Arg131 and Glu268 during free MD simulation. After 0.5 ns, the Glu/Arg ion pair loses its connection.

Asn51 in helix I and Ser319 in helix VII, as can be seen in Fig. 3A. This bond creates a stable hydrophilic connection between helices I and VII. The ionic lock, involving the highly conserved E/DRY motif in helix III [5], opens during free MD simulation in nice agreement with the X-ray structure (Fig. 3B): after 0.5 ns, Arg131 (helix III) loses its connection to Glu268 (helix VI) because of electrostatic interaction with Asp130.

3.4. Ligand binding site

The ligand binding site in the X-ray and the simulated model is shown in Fig. 4. The B2AR model shows only one cavity

within the protein large enough to accommodate the native ligand epinephrine. Residues known to be involved in ligand binding [20] are found at the surface of the cavity. Its location and form fit well the demands of epinephrine, and is comparable to the one in 2RH1. Deviations in its form are due to a different boundary formed by e12 in our model and the crystal structure, respectively: while in the crystal structural model 2RH1, the niche is open to the extracellular medium, it is closed completely by the loop in the simulated model. However there is a high correspondence in the positions of the ligands. The small differences observed may also be related to

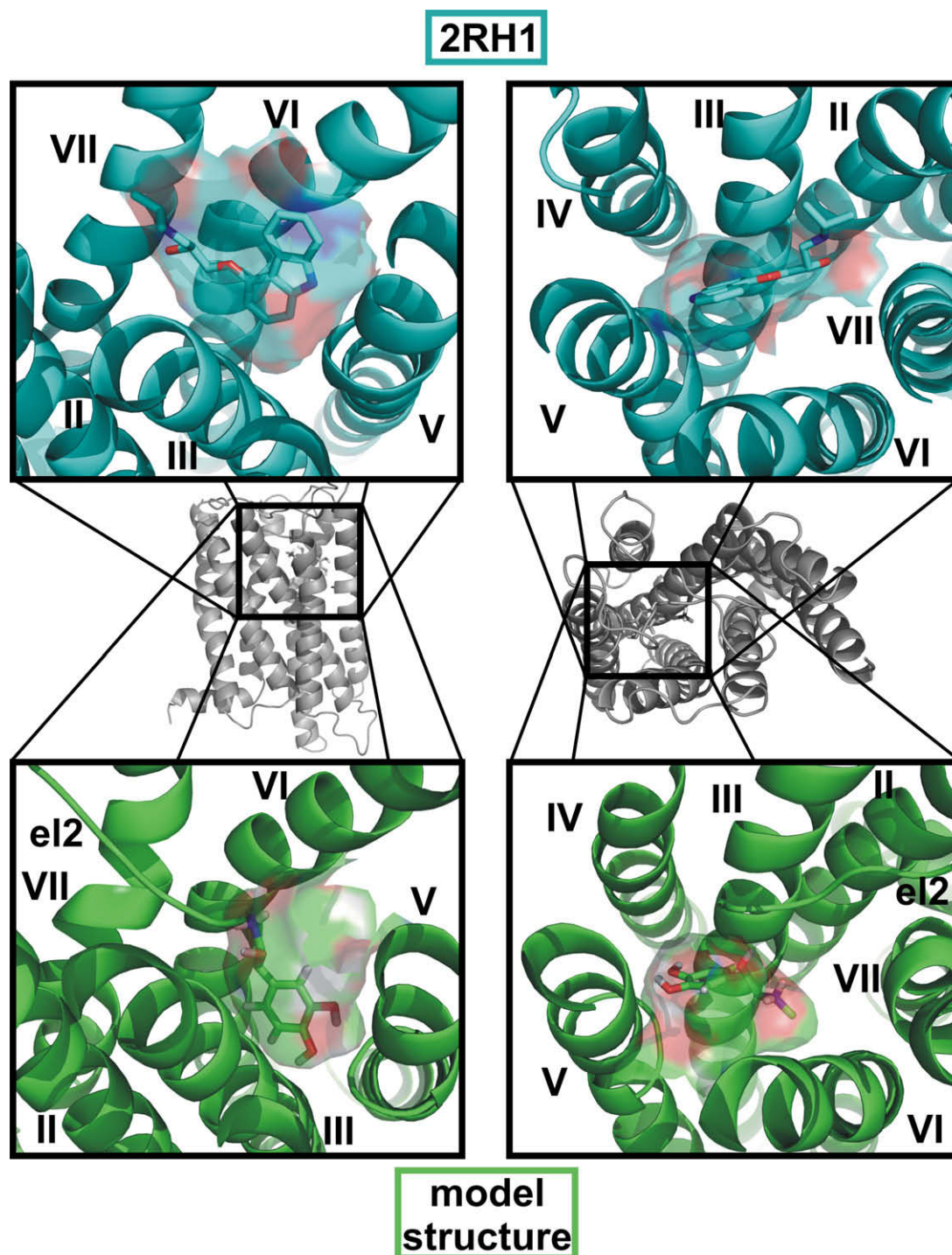


Fig. 4. Protein surface of the binding pocket of B2AR in perpendicular view. Top: crystal structure 2RH1. Carazolol shown in sticks. Bottom: dynamic model after 10 ns. Epinephrine shown in sticks. The binding pocket in the model is comparable by location and form to the one in 2RH1.

the effect of the respective ligand on the receptor: while epinephrine used in the model is an agonist, carazolol in the crystal structural model is a partial inverse agonist, which might bind in a slightly different mode. We therefore focus on a detailed evaluation of the binding mode of epinephrine observed in our B2AR model. Note that docking of the agonist isoproterenol into 2RH1 [26] did not result in a reasonable binding mode, so 2RH1 might be a less suited target for analysis of agonist binding in b2ar.

Fig. 5 shows the contact pattern between epinephrine and B2AR during free MD simulation and a representative binding structure after 10 ns of simulation. Epinephrine forms hydrophobic contacts to Val114, Phe289, and Phe290, and hydrogen bonds to Asp113, Asn293, Ser203, Ser204, and Ser207. All residues are known from point mutation analysis and are proposed to interact with epinephrine [20,39,40]. Concerning the predicted dynamics of those contacts: epinephrine loses its initial contacts to Ser207 and Asn293 during the first 0.1 ns. After

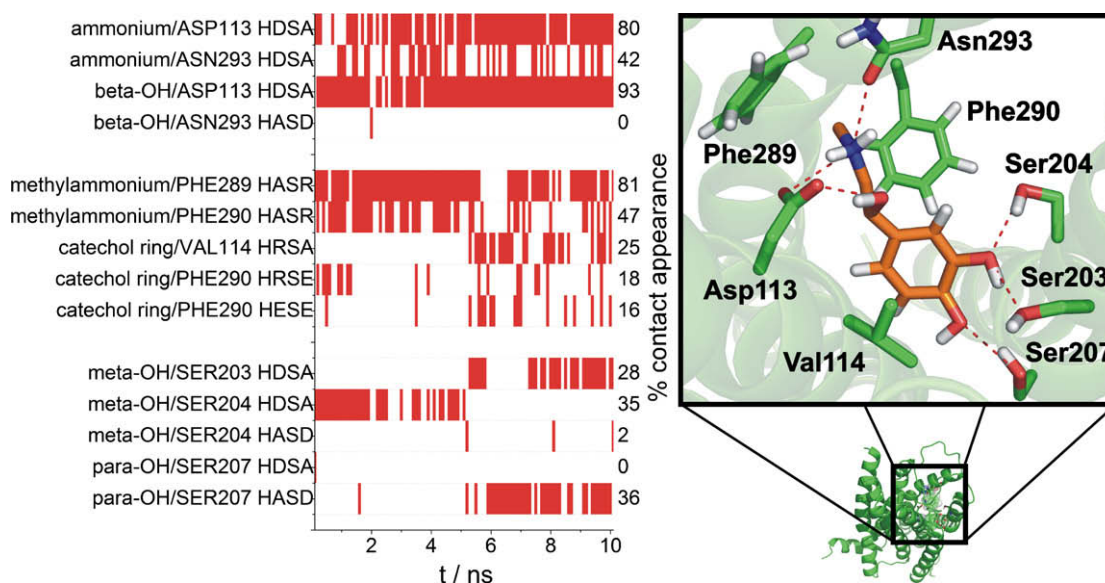


Fig. 5. Ligand binding in dynamic homology model. Left: Contact analysis of receptor model and epinephrine. A: alkyl group or acceptor contact; B: protein backbone contact; D: donor contact; E: contact on edge of ring; H: hetero group (epinephrine); R: contact on ring plane; S: amino acid side chain. Epinephrine ammonium moiety and β hydroxyl group contacts remain stable during simulation. The terminal methyl moiety is intercalated between Phe289 and Phe290. After 5 ns, the catechol ring forms contacts to Val114 and Phe290. The catechol hydroxyl group bond pattern changes after 5 ns. Right: representative binding mode of epinephrine at 10 ns of free MD simulation. Epinephrine in orange. Epinephrine forms hydrophobic contacts to Val114, Phe290, and Phe290, and hydrophilic contacts to Asp113, Asn293, Ser203, Ser204, and Ser207.

5 ns, the catechol ring of epinephrine flips to a position where it is sandwiched between Val114 and Phe290. The terminal methyl moiety forms a stable van der Waals contact with the phenyl rings of Phe289 and Phe290. Unlike in the starting structure, Asn293 forms a hydrogen bond to the ammonium moiety instead of the β hydroxyl group of epinephrine, which engages in a hydrogen bond with Asp113, attaching the ligand in a clamp-like manner to the carboxylic residue. Ser203 and Ser207 form hydrogen bond contacts to the *meta* and *para* hydroxyl groups of epinephrine, respectively, while Ser204 binds occasionally to the *meta* hydroxyl group.

4. Discussion

While developing our modelling technique before the publication of the b2ar crystal structures, we appreciate the nice agreement between our model and the crystal structure during simulation (see Figs. 1 and 2). The dynamic model is particularly accurate at reproducing the 7TM domains, and the ligand binding site. The flexible loops show larger deviations, and e12, which shows the largest deviation between rhodopsin and b2ar, together with the intramolecular disulphide bond pattern is not well predicted. However, the deviations between the modelled and the X-ray structure are mostly related to inter-protein contacts observed in the crystal.

With respect to dynamic properties, a more detailed comparison shows that the contact of Asn51 and Ser319 connecting helices I and VII is continuously maintained. This contact can also be observed in the crystal structural model [6]. It was already reported to be stable in MD simulations on rhodopsin and is believed to be an important and conserved connection motif of GPCRs [9]. Asn51 is the most conserved residue in Helix I [23]. Point mutation studies on the analogous α_{1B} -adrenergic receptor [41] demonstrated that a mutation to

Ala results in a constitutively active receptor, while mutation to Asp, which can exhibit the observed hydrogen bond as well, did not have an impact on the receptor function. The hydrogen bond therefore seems to be important for differentiating between active and inactive conformation of the receptor.

The salt bridge formed between Asp130 and Arg131 is important for keeping the receptor in an inactive state. It is ruptured via a protonation of Asp130 upon receptor activation. Mutation of Asp130 to Asn shows an increase in basal activity of the receptor [42], and Arg131 is a key residue for G protein binding [24]. The opening of the salt bridge between Arg131 and Glu268, a feature found in the X-ray structures of the β_2 adrenergic receptor [5,6] but not in rhodopsin, is accurately predicted in the simulated model. Interestingly, point mutation analysis shows that mutation of Glu268 to Gln or Ala results in a constitutively active receptor, which was interpreted to be related to an interaction between Asp130/Arg131 and Glu268 [42]. Crystal structures and simulation alike point to a weakening of this interaction in b2ar compared to rhodopsin. It seems to be related to the basal activity of b2ar, while rhodopsin does not exhibit such activity in the inactive state [5].

As can be seen in Fig. 4, the ligand binding niche is also well predicted. The behaviour of (–)-epinephrine during simulation (shown in Fig. 5) is remarkable: although (–)-epinephrine was docked into a model derived from rhodopsin in an inactive conformation, epinephrine fits well into the cavity appearing during model building in its lowest-energy conformation. The reorientation after 5 ns positions the ligand into a binding mode which agrees well with point mutation analysis and ligand binding assays. Epinephrine establishes the proposed hydrogen bond pattern with Serines 203, 204 and 207 mentioned in Ref. [43]. The significance of hydrophobic contacts to Phe289 and Phe290 for agonist binding is confirmed by point mutation analysis [40]. Val114 is highly conserved in

the adrenergic receptor family, and mutation to Ala leads to a 300-fold loss of agonist affinity compared to a 3-fold loss of antagonist affinity [39]. The clamp-like connection of ammonium group, β hydroxyl group and Asp113 side chain with Asn293 bonded to the ammonium group explains point mutation data on Asn293 [44] in a way not yet reported. A switch of enantiomer would interfere with the connection to both Asp113 and Asn293. Mutation of Asn293 to leucine and subsequent loss of a connecting hydrogen bond would affect binding negatively as well. Furthermore, mutation of Asn293 to Asp would put a negatively charged residue close to Asp113 and perturb the binding pattern necessary for receptor activation, which offers an explanation to the data in Ref. [45]. A similar ring-like mode can be seen in 2RH1 between carazolol and Asp113 (see Fig. 4D in Ref. [26]). Docking of epinephrine into the protein model therefore leads to a dynamic binding mode which is in agreement with data on ligand binding during free MD simulation.

5. Conclusions

During free MD simulation, our dynamic homology model of B2AR reproduces structural and dynamic properties which are reported for the X-ray structural model. The model exhibits a cavity which meets the sterical and electrostatic demands of the native agonist epinephrine, which binds to the protein in a stable binding mode during simulation. Therefore, GPCR models created this way can be used to gain insight into protein structure, and receptor/ligand binding dynamics which are not accessible by static homology models.

Acknowledgements: The authors would like to thank the NIC Jülich (Project No. hbo26) and the RRZK Köln for providing computing time, and the Ruhr-University Research School for additional funding. They are also grateful to Ulrike Krüger and Keith Heysmond for improving the English of the manuscript. All molecular images were produced with PyMOL [46].

Appendix A. Supplementary data

Supplementary data associated with this article can be found, in the online version, at doi:10.1016/j.febslet.2008.08.022.

References

- [1] Pierce, K.L., Premont, R.T. and Lefkowitz, R.J. (2002) Seven-transmembrane receptors. *Nature Rev.* 3, 639–650.
- [2] Lundstrom, K. (2006) Latest development in drug discovery on G protein-coupled receptors. *Curr. Protein Pept. Sci.* 7, 465–470.
- [3] Palczewski, K., Kumasaka, T., Hori, T., Behnke, C.A., Motoshima, H., Fox, B.A., Le Trong, L., Teller, D.C., Okada, T., Stenkamp, R.E., Yamamoto, M. and Miyano, M. (2000) Crystal structure of rhodopsin: a G-protein coupled receptor. *Science* 289, 739–745.
- [4] Okada, T., Sugihara, M., Bondar, A.N., Elstner, M., Entel, P. and Buss, V. (2004) The retinal conformation and its environment in rhodopsin in light of a new 2.2 Å crystal structure. *J. Mol. Biol.* 342, 571–583.
- [5] Rasmussen, S.G., Choi, H.J., Rosenbaum, D.M., Kobilka, T.S., Thian, F.S., Edwards, P.C., Burghammer, M., Ratnala, V.R., Sanishvili, R., Fischetti, R.F., Schertler, G.F., Weis, W.I. and Kobilka, B.K. (2007) Crystal structure of the human beta(2) adrenergic G-protein-coupled receptor. *Nature* 450, 383–387.
- [6] Cherezov, V., Rosenbaum, D.M., Hanson, M.A., Rasmussen, S.G., Thian, F.S., Kobilka, T.S., Choi, H.J., Kuhn, P., Weis, W.I., Kobilka, B.K. and Stevens, R.C. (2007) High-resolution crystal structure of an engineered human beta(2)-adrenergic G protein coupled receptor. *Science* 318, 1258–1265.
- [7] Ballesteros, J. and Palczewski, K. (2001) G protein-coupled receptor drug discovery: Implications from the crystal structure of rhodopsin. *Curr. Opin. Drug Discov. Dev.* 4, 561–574.
- [8] Ballesteros, J.A., Shi, L. and Javitch, J.A. (2001) Structural mimicry in G protein-coupled receptors: implications of the high-resolution structure of rhodopsin for structure-function analysis of rhodopsin-like receptors. *Mol. Pharmacol.* 60, 1–19.
- [9] Schlegel, B., Sippl, W. and Höltje, H.D. (2005) Molecular dynamics simulations of bovine rhodopsin: influence of protonation states and different membrane-mimicking environments. *J. Mol. Model.* 12, 49–64.
- [10] Huber, T., Botelho, A.V., Beyer, K. and Brown, M.F. (2004) Membrane model for the G-protein-coupled receptor rhodopsin: hydrophobic interface and dynamical structure. *Biophys. J.* 86, 2078–2100.
- [11] Bissantz, C., Bernard, P., Hilbert, M. and Rognan, D. (2003) Protein-based virtual screening of chemical databases. II. Are homology models of G protein-coupled receptors suitable targets? *Proteins: Struct. Funct. Genet.* 50, 5–25.
- [12] Furse, K.E. and Lybrand, T.P. (2003) Three-dimensional models for β -adrenergic receptor complexes with agonists and antagonists. *J. Med. Chem.* 46, 4450–4462.
- [13] Freddolino, P.L., Kalani, M.Y.S., Vaidehi, N., Floriano, W.B., Hall, S.E., Trabanino, R.J., Kam, V.W.T.K. and Goddard III, W.A. (2004) Predicted 3D structure for the human β 2-adrenergic receptor and its binding site for agonists and antagonists. *Proc. Natl. Acad. Sci. USA* 101, 2736–2741.
- [14] Gouldson, P.R., Kidley, N.J., Bywater, R.P., Psaroudakis, G., Brooks, H.D., Diaz, C., Shire, D. and Reynolds, C.A. (2004) Toward the active conformations of rhodopsin and the β 2-adrenergic receptor. *Proteins: Struct. Funct. Bioinform.* 56, 67–84.
- [15] Spijker, P., Vaidehi, N., Freddolino, P.L., Hilbers, P.A.J. and Goddard III, W.A. (2006) Dynamic behavior of fully solvated β 2-adrenergic receptor, embedded in the membrane with bound agonist or antagonist. *Proc. Natl. Acad. Sci. USA* 103, 4882–4887.
- [16] Ivanov, A.A., Fricks, I., Harden, T.K. and Jacobson, K.A. (2006) Molecular dynamics simulation of the P2Y14 receptor ligand docking and identification of a putative binding site of the distal hexose moiety. *Bioorg. Med. Chem. Lett.* 17, 761–766.
- [17] Hallmen, C. and Wiese, M. (2006) Molecular dynamics simulation of the human adenosine A(3) receptor: agonist induced conformational changes of Trp243. *J. Comput. Aided Mol. Des.* 20, 673–684.
- [18] Rivail, L., Chipot, C., Maigret, B., Bestel, I., Sicsic, S. and Tarek, M. (2007) Large-scale molecular dynamics of a G protein-coupled receptor, the human 5-HT4 serotonin receptor, in a lipid bilayer. *Theochem* 817, 19–26.
- [19] Espinoza-Fonseca, L.M., Pedretti, A. and Vistoni, G. (2008) Structure and dynamics of the full-length M1 muscarinic acetylcholine receptor studied by molecular dynamics simulations. *Arch. Biochem. Biophys.* 469, 142–150.
- [20] Swaminanth, G., Xiang, Y., Lee, T.W., Steenhuis, J., Parnot, C. and Kobilka, B.K. (2004) Sequential binding of agonists to the β 2 adrenoceptor. *J. Biol. Chem.* 279, 686–691.
- [21] Altschul, S.F., Madden, T.L., Schäffer, A.A., Zhang, J., Zhang, Z., Miller, W. and Lipman, D.J. (1997) Gapped BLAST and PSI-BLAST: a new generation of protein database search programs. *Nucleic Acids Res.* 25, 3389–3402.
- [22] Higgins, D., Thompson, J., Gibson, T., Thompson, J.D., Higgins, D.G. and Gibson, T.J. (1994) CLUSTAL W: improving the sensitivity of progressive multiple sequence alignment through sequence weighting, position-specific gap penalties and weight matrix choice. *Nucleic Acids Res.* 22, 4673–4680.
- [23] Ballesteros, J.A. and Weinstein, H. (1995) Integrated methods for the construction of three-dimensional models and computational

- probing of structure–function relations in G protein coupled receptors. *Meth. Neurosci.* 25, 366–428.
- [24] Gether, U. (2000) Uncovering molecular mechanisms involved in activation of G protein-coupled receptors. *Endocr. Rev.* 21, 90–113.
- [25] Kim, J.-M., Hwa, J., Garriga, P., Reeves, P.J., RajBhandary, U.L. and Khorana, H.G. (2005) Light-driven activation of β_2 -adrenergic receptor signaling by a chimeric rhodopsin containing the β_2 -adrenergic receptor cytoplasmic loops. *Biochemistry* 44, 2284–2292.
- [26] Rosenbaum, D.M., Cherezov, V., Hanson, M.A., Rasmussen, S.G.F., Thian, F.S., Kobilka, T.S., Choi, H.-J., Yao, X.-J., Weis, W.I., Stevens, R.C. and Kobilka, B.K. (2007) GPCR engineering yields high-resolution structural insights into β_2 -adrenergic receptor function. *Science* 318, 1266–1273.
- [27] Rands, E., Candelore, M.R., Cheung, A.H., Hill, W.S., Strader, C.D. and Dixon, R.A.F. (1990) Mutational analysis of β -adrenergic receptor glycosylation. *J. Biol. Chem.* 265, 10759–10764.
- [28] Canutescu, A.A., Shelenkov, A.A. and Dunbrack Jr., R.L. (2003) A graph-theory algorithm for rapid protein side-chain prediction. *Protein Sci.* 12, 2001–2014.
- [29] Höweler, U. (2007) MAXIMOBY 8.1 and MOBY 3.0, CHEOPS, Altenberge, Germany.
- [30] Frisch, M.J., Trucks, G.W., Schlegel, H.B., Scuseria, G.E., Robb, M.A., Cheeseman, J.R., Montgomery, Jr., J.A., Vreven, T., Kudin, K.N., Burant, J.C., Millam, J.M., Iyengar, S.S., Tomasi, J., Barone, V., Mennucci, B., Cossi, M., Scalmani, G., Rega, N., Petersson, G.A., Nakatsuji, H., Hada, M., Ehara, M., Toyota, K., Fukuda, R., Hasegawa, J., Ishida, M., Nakajima, T., Honda, Y., Kitao, O., Nakai, H., Klene, M., Li, X., Knox, J.E., Hratchian, H.P., Cross, J.B., Bakken, V., Adamo, C., Jaramillo, J., Gomperts, R., Stratmann, R.E., Yazyev, O., Austin, A.J., Cammi, R., Pomelli, C., Ochterski, J.W., Ayala, P.Y., Morokuma, K., Voth, G.A., Salvador, P., Dannenberg, J.J., Zakrzewski, V.G., Dapprich, S., Daniels, A.D., Strain, M.C., Farkas, O., Malick, D.K., Rabuck, A.D., Raghavachari, K., Foresman, J.B., Ortiz, J.V., Cui, Q., Baboul, A.G., Clifford, S., Cioslowski, J., Stefanov, B.B., Liu, G., Liashenko, A., Piskorz, P., Komaromi, I., Martin, R.L., Fox, D.J., Keith, T., Al-Laham, M.A., Peng, C.Y., Nanayakkara, A., Challacombe, M., Gill, P.M.W., Johnson, B., Chen, W., Wong, M.W., Gonzalez, C. and Pople, J.A. (2004). Gaussian 03, Revision C.02. Gaussian Inc., Wallingford CT, USA.
- [31] Burisch, C., Wildner, G.F. and Schlitter, J. (2007) Bioinformatic tools uncover the C-terminal strand of Rubisco's large subunit as hot-spot for specificity-enhancing mutations. *FEBS Lett.* 581, 741–748.
- [32] Van der Spoel, D., Lindahl, E., Hess, B., Groenhof, G., Mark, A.E. and Berendsen, H.J.C. (2005) GROMACS: fast, flexible, and free. *J. Comput. Chem.* 26, 1701–1718.
- [33] Berger, O., Edholm, O. and Jahnig, F. (1997) Molecular dynamics simulations of a fluid bilayer of dipalmitoylphosphatidylcholine at full hydration, constant pressure, and constant temperature. *Biophys. J.* 72, 2002–2013.
- [34] Tieleman, D.P., Sansom, M.S.P. and Berendsen, H.J.C. (1999) Alamethicin helices in a bilayer and in solution: molecular dynamics simulations. *Biophys. J.* 73, 2376–2392.
- [35] Fahmy, K., Jäger, F., Beck, M., Zvyaga, T.A., Sakmar, T.P. and Siebert, F. (1993) Protonation states of membrane-embedded carboxylic acid groups in rhodopsin and metarhodopsin II: a Fourier-transform infrared spectroscopy study of site-directed mutants. *Proc. Natl. Acad. Sci. USA* 90, 10206–10210.
- [36] Schuettelkopf, A.W. and van Aalten, D.M.F. (2004) PRODRG—a tool for high-throughput crystallography of protein-ligand complexes. *Acta Crystallogr. D60*, 1355–1363.
- [37] Kandt, C., Schlitter, J. and Gerwert, K. (2004) Dynamics of water molecules in the bacteriorhodopsin trimer in explicit lipid/water environment. *Biophys. J.* 86, 705–714.
- [38] Dohlman, H.G., Caron, M.G., DeBlasi, A., Frielle, T. and Lefkowitz, R.J. (1990) Role of extracellular disulphide-bonded cysteines in the ligand binding function of the β_2 -adrenergic receptor. *Biochemistry* 29, 2335–2342.
- [39] Chelikani, P., Hornak, V., Eilers, M., Reeves, P.J., Smith, S.O., RajBhandary, U.L. and Khorana, H.G. (2007) Role of group-conserved residues in the helical core of β_2 -adrenergic receptor. *Proc. Natl. Acad. Sci. USA* 104, 7027–7032.
- [40] Strader, C.D., Sigal, I.S. and Dixon, R.A.F. (1989) Structural basis of β -adrenergic receptor function. *FASEB J.* 3, 1825–1832.
- [41] Scheer, A., Fanelli, F., Costa, T., De Benedetti, P.G. and Cotecchia, S. (1996) Constitutively active mutants of the α_1B -adrenergic receptor: role of highly conserved polar amino acids in receptor activation. *EMBO J.* 15, 3566–3578.
- [42] Ballesteros, J.A., Jensen, A.D., Liapakis, G., Rasmussen, S.G.F., Shi, L., Gether, U. and Javitch, J.A. (2001) Activation of the β_2 -adrenergic receptor involves disruption of an ionic lock between the cytoplasmic ends of transmembrane segments 3 and 6. *J. Biol. Chem.* 276, 29171–29177.
- [43] Liapakis, G., Ballesteros, J.A., Papachristou, S., Chan, W.C., Chen, X. and Javitch, J.A. (2000) The forgotten serine. *J. Biol. Chem.* 275, 37779–37788.
- [44] Wieland, K., Zuurmond, H.M., Andexinger, S., IJzerman, A.P. and Lohse, M.J. (1996) Involvement of Asn-293 in stereospecific agonist recognition and in activation of the β_2 -adrenergic receptor. *Proc. Natl. Acad. Sci. USA* 93, 9276–9281.
- [45] Hannawacker, A., Krasel, C. and Lohse, M. (2002) Mutation of Asn293 to Asp in transmembrane helix VI abolishes agonist-induced but not constitutive activity of the β_2 -adrenergic receptor. *Mol. Pharmacol.* 62, 1431–1437.
- [46] DeLano, W.L. (2002) The PyMOL Molecular Graphics System, DeLano Scientific, Palo Alto, CA, USA.